INTERACTION MODEL BETWEEN AN ELECTRICAL ARC AND A MATERIAL: WELDING TIG APPLICATION

J. MOUGENOT*, J.-J. GONZALEZ, P. FRETON AND M. MASQUÈRE

Université de Toulouse ; UPS, CNRS, INPT ; LAPLACE (Laboratoire Plasma et Conversion d'Energie UMR 5213) ; 118 route de Narbonne, F-31062 Toulouse cedex 9, France
*jonathan.mougenot@laplace.univ-tlse.fr

ABSTRACT

The paper aim is to study the influence of the current path in a metal work-piece of a welding Tungsten Inert Gas (TIG) configuration. A transient three-dimensional and magneto-hydrodynamic model of an interaction between an electrical arc and a metal work-piece is presented. The model couples the plasma and the metal domains and takes into account the metallic vapours presence.

1. INTRODUCTION

Thermal plasmas are used in several industrial applications as spraying, cutting, TIG welding. For this last application, an electric arc is established in an inert gas between a non-fusible tungsten electrode and the metallic work piece connected to the power supply by a mass clip. The thermal plasma, created by the arc, transfers its energy to the metal leading to the creation of a melted zone and production of metallic vapours. The process quality (as depth-to-width ratio) depends on the arc properties.

The arc shape is due to the convection, the magnetic force and the pressure gradient [1]. Several authors studied the magnetic arc deviation. Gonzalez *et al* [2] studied the deflection due to a magnetic field created by the current intensity circulation in a conductive wire closed to the arc. Yin *et al* [3] described the deformation due to the presence of an axial magnetic field created by an exciting coil placed all around the cathode. Yamamoto *et al* [4] showed the impact of the coil presence all around the work-piece. An arc deviation is also reported when the mass clip position is asymmetric [5]. However, to our knowledge, no simulation of this phenomenon is available in the literature. In order to quantify this phenomenon a transient three-dimensional model of an electrical arc in interaction with a metal work-piece [6] is used.

The model solves the magneto-hydrodynamics equations to describe the plasma and the metal part taking into account the liquid-solid phase change and the vapour production. Four forces acts on the liquid metal: the Marangoni force (with a Marangoni coefficient depending on temperature), the drag force, the electromagnetic force and the gravity. The model was developed from the code @Saturne [7] distributed in GPL license by EDF and based on the finite-volume method. Several modifications of the code were necessaries to take into account the interfacing between the plasma and the material as well as the resolution of the physical phenomena in the melted zone [8].

The physical bases of the model are presented in a first part. Next, the model is applied for a configuration closed to a TIG welding conditions: Arcal.37 plasma (70%mol He and 30%mol Ar) in interaction with an AISI 304 work-piece (with 200pmm of sulphur content). The applied current intensity is I=200 A and the arc length d=5.5 mm. Two configurations are compared: one with a symmetric return current connection to the work piece and the other with an asymmetric return current connection.

2. MODEL DESCRIPTION

The following conditions and assumptions are adopted:

- The weld pool surface is not deformable.
- The welding torch is stationary.
- The plasma and anode metal are solved in a same calculation domain. The cathode domain is not solved.

- The plasma and the weld pool are considered as Newtonian fluids.
- The plasma is at LTE and the flow is laminar.
- The weld pool flow is assumed laminar.

The conservation laws of the magneto-hydrodynamics are solved for the plasma and metal parts in a same 3D cylindrical domain.

Mass conservation:

$$\frac{\partial \rho}{\partial t} + \nabla \cdot (\rho \mathbf{v}) = 0 \tag{1}$$

ρ is the mass density and $\mathbf{v}$ the velocity vector.

Momentum conservation:

$$\frac{\partial \rho \mathbf{v}}{\partial t} + \nabla \cdot (\rho \mathbf{v} \otimes \mathbf{v}) = -\nabla p + \nabla \cdot \tau + \mathbf{j} \times \mathbf{B} + \rho \mathbf{g} + \mathrm{TS} \tag{2}$$

p is the pressure, g is the standard acceleration of gravity, $\mathbf{j}$ the current density and $\mathbf{B}$ the magnetic field deduced from vector potential equations and τ the shear stress. On weld pool surface, additional source terms TS are included to represent the two superficial forces:

- The Marangoni force:

$$\mathrm{TS}_i = \frac{\partial}{\partial z}\left[\frac{\partial \gamma}{\partial T}\frac{T}{\partial i}\right] \tag{3}$$

  i represents the tangent contribution of the axial components (x and y) and T is the temperature. The Marangoni coefficient $\partial\gamma/\partial T$ is taken as a function of temperature with sulphur as active component.

- The drag force:

$$\mathrm{TS} = \frac{\partial}{\partial z}\left[\eta \left.\frac{\partial v}{\partial z}\right|_p - \eta \left.\frac{\partial v}{\partial z}\right|_a\right] \tag{4}$$

  p and a represent respectively the plasma and anode parts.

Enthalpy conservation:

$$\frac{\partial \rho h}{\partial t} + \nabla \cdot (\rho \mathbf{v} h) = \nabla\left(\frac{\lambda}{c_p}\nabla h\right) + \frac{\mathbf{j}\cdot\mathbf{j}}{\sigma} + \mathrm{TS} \tag{5}$$

h is the static enthalpy, λ is the thermal conductivity, c_p is the specific heat capacity and σ is the electrical conductivity.

Specific terms are added for plasma: enthalpic transport of the electron and radiation losses:

$$\mathrm{TS} = \frac{5k_b}{2e}\nabla \cdot \left(\frac{h}{c_p}\mathbf{j}\right) - 4\pi\epsilon_n \tag{6}$$

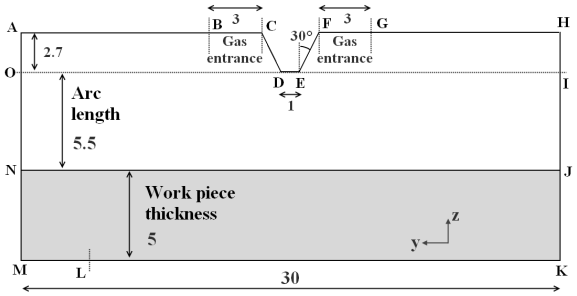

Fig. 1: *Geometry in (y-z) section (distance in mm).*

Tab. 1: *Boundary conditions. (*) For the reference case.*

Zone	$\mathbf{v}$ (m s^{-1})	$\mathbf{T}$ (K)	$\mathbf{V}$ (U)	$\mathbf{A}$ (T m)
AB-GH	$\nabla(\rho\mathbf{v})\cdot\mathbf{e}_n = 0$	$\nabla T\cdot\mathbf{e}_n = 0$	$\nabla V\cdot\mathbf{e}_n = 0$	$\nabla A\cdot\mathbf{e}_n = 0$
BC-FG	$\rho\mathbf{v} = 10\text{nl min}^{-1}$	$T = 300$	$\nabla V\cdot\mathbf{e}_n = 0$	$\nabla A\cdot\mathbf{e}_n = 0$
CDEF	$\rho\mathbf{v} = 10\text{nl min}^{-1}$	$T = 3500$	$\nabla V\cdot\mathbf{e}_n = 0$	$\nabla A\cdot\mathbf{e}_n = 0$
HJ-MN	$\nabla(\rho\mathbf{v})\cdot\mathbf{e}_n = 0$	$\nabla T\cdot\mathbf{e}_n = 0$	$\nabla V\cdot\mathbf{e}_n = 0$	$A = 0$
HJ-MN	$\mathbf{v} = 0$	$T = 300$	$V = 0$ (*)	$A = 0$
HJ-MN	$\mathbf{v} = 0$	$T = 300$	$V = 0$ (*)	$\nabla A\cdot\mathbf{e}_n = 0$

e is the elementary charge, k_b the Boltzmann constant and ϵ_n represents the net emission coefficient.

At the interface between the plasma and the workpiece (as an anode), the anode flux q_a is equal to:

$$q_a = q_{cond.} + |j_z|\frac{\phi_a}{e} - L_{mat}\phi_v \tag{7}$$

$q_{cond.}$ represents the conduction flux, ϕ_a is the electron work function (taken equal to 4.7 eV), L_{mat} is the latent heat of gasification (taken equal to $73.43{\cdot}10^4$ J.kg^{-1}) and ϕ_v the evaporation flux of metal vapours.

Electrical potential equation:

$$\nabla \cdot (\sigma \nabla V) = 0 \tag{8}$$

The electrical field $\mathbf{E}$ and the current density $\mathbf{j}$ is deduced from the electrical potential with a simple Ohm's law:

$$\mathbf{j} = \sigma\mathbf{E} = -\sigma\nabla V \tag{9}$$

Vector potential equations - Magnetic field:

$$\nabla \cdot (\nabla \mathbf{A}) = -\mu_0 \mathbf{j} \tag{10}$$

μ_0 is the vacuum permeability. Resolving this equation yields the magnetic field:

$$\mathbf{B} = \nabla \times \mathbf{A} \tag{11}$$

Mass fraction conservation:

$$\frac{\partial \rho Y_m}{\partial t} + \nabla \cdot (\rho \mathbf{v} Y_m) = \nabla\left(\rho D \nabla Y_m\right) + \mathrm{TS} \tag{12}$$

Y_m represents the mass fraction of metallic vapours. We assume that the diffusion coefficient $D = \eta/\rho$ (according to the Schmidt number equal to 1).

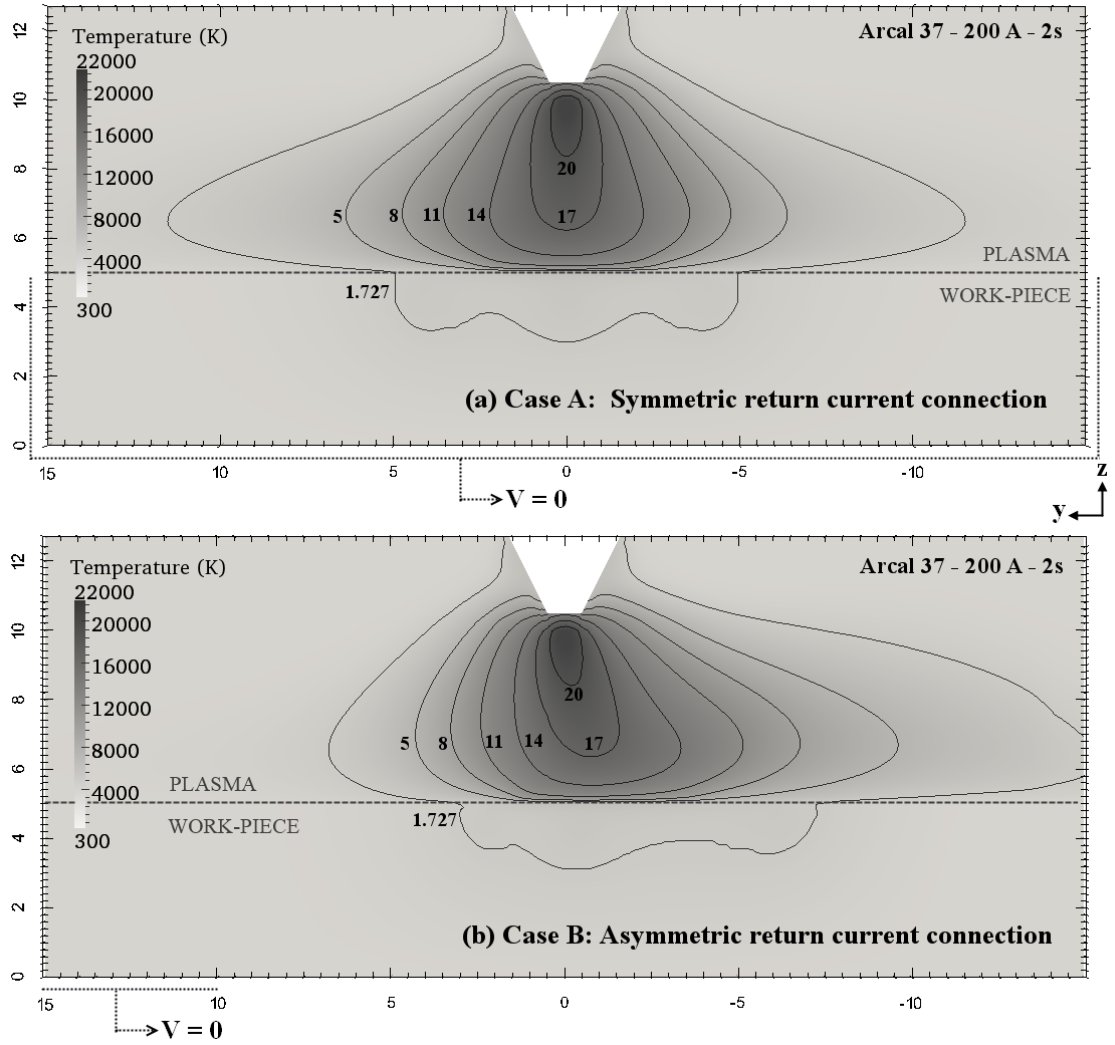

Fig. 2: *Temperatures for the 2 cases in (y,z) section. Isotherms in kK. Distance in mm.*

Based on pure properties components, the local plasma properties are calculated with mixtures laws [6] depending on the local vapour concentrations and temperature. The vapour production is imposed with a source term in the first cells above the anode. On weld pool surface:

$$Y_m = \frac{P_v M_m}{P_v M_m + (P_0 - P_v) M_p} \tag{13}$$

M_m and M_p are respectively the molar mass of metal and plasma, P_0 the atmospheric pressure and P_v the pressure vapour of metal.

Fig. 1 shows the geometry and Tab. 1 presents the boundary conditions. The current polarity is direct: the tungsten electrode (CDEF) is the cathode and the work-piece (NJKM) is the anode. Current density is imposed below the cathode as an exponential profile:

$$j_z = j_{max} \exp\left(-b\sqrt{x^2 + y^2}\right) \tag{14}$$

j_{max} is equal to 1.2·108 A.m^{-2} and the parameter b is deduced from intensity:

$$I = 2\pi \int_0^{R_c} j(r) r dr \tag{15}$$

R_c is the conduction radius of the electrical arc (taken equal to 2 mm).

3. RESULTS

The model is applied to study the arc deviation due to the position of the return current connection. Two cases are presented in this section:

- Case A (reference case): the electrical voltage boundary is equal to 0 for all the anode part (Fig.1: NJKN). For this case the return current connection is symmetric.
- Case B: the voltage anode boundary is equal to 0 only in a part of the anode (Fig.1: LM; x <5 mm and y >10 mm). For this case the return current connection is asymmetric.

Fig. 2 presents the temperature field in a (y-z) section after 2 s of interaction for the 2 cases (isotherms in kK). In metal part, the 1727 K isotherm corresponds to solid-liquid phase change.

For the 3D case A (Fig. 2(a)), the results present a natural symmetry due to the fact that the physicals phenomena described are symmetric. Thus the weld pool dimensions are symmetric: the width is equal to 9.9 mm and the depth is equal to 1.9 mm. The weld pool volume is 103 mm^3.

In comparison with the case A, the case B isotherms (Fig. 2(b)) are moved towards the y negative values: for example the isotherm 8 kK extends from y=-7.7 mm to y=-3.3 mm as there are located between [-5; 5] for the case A. The weld pool width (10.3 mm) and depth (1.9 mm) are close to the case A but it is more extended to the y negative values and the molten volume is reduced (89 mm^3). We notice that the plasma and the weld pool are deflected in the opposite direction of the position of the current connection (which represents the mass clip).

Fig. 3 presents the norm of current density in the whole calculation domain. The down part of the figure corresponds to the material as the upper part is the plasma medium. In the left side of the figure 3 in the material domain the current density is higher than in the anode center. The vector current density is oriented to the right and that it is parallel to the anode surface. This current circulation in the material leads to a magnetic field equal to 20 mT which modifies the current circulation in the vicinity of the anode-plasma interface leading to a plasma deviation. The temperature field is so deformed and deviated breaking the natural symmetry. Changes are also observed on the electromagnetic forces and so, on the molten zone.

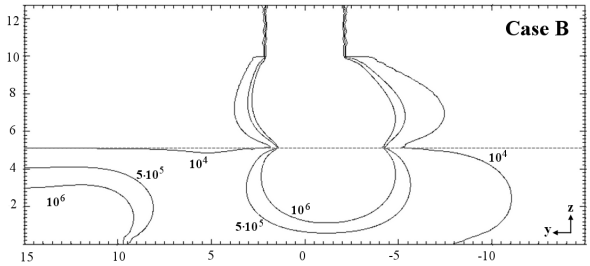

Fig. 3: *Current density contours (values in A.m^{-2}) for case B in (y-z) section. Distance in mm.*

4. CONCLUSION

Based on @Saturne a 3D model describing on the whole domain the plasma and the material was built. The model previously validated allows parametric studies on several quantities and a better understanding of the forces acting on the weld pool.

In this paper the influence of the current path in the material on the plasma behaviour is clearly demonstrated showing all the importance of well describing the current circulation for a better improvement of the process.

REFERENCES

[1] R. P. Reis, D. Souza and A. Scotti, "Models to describe plasma jet, arc trajectory and arc blow formation in arc welding", Welding in the world, 55, 24-32, 2011.

[2] J.-J. Gonzalez, F. Lago, P. Freton *et al*, "Numerical modelling of an electric arc and its interaction with the anode: part II. The three-dimensional model-influence of external forces on the arc column", J. Phys. D: App. Phys., 38, 306-318, 2005.

[3] X. Yin, J. Gou, J. Zhang *et al*, "Numerical study of arc plasmas and weld pools for GTAW with applied axial magnetic fields", J. Phys. D: App. Phys., 45, 285203, 2012.

[4] Y. Yamamoto, K. Iwai and S. Asai, "Plasma Behavior under Imposition of Alternating Magnetic Field Perpendicular or Parallel to the Plasma Arc Current", ISIJ International, 47, 960-64, 2007.

[5] K. Weman, *Welding processes*, Woodhead Publishing Ltd, 196, 2003.

[6] J. Mougenot, J.-J. Gonzalez, P. Freton *et al*, "Argon and Arcal.37 plasma characteristics in a TIG configuration", J. Phys. D: App. Phys., 46, 495203, 2013.

[7] F. Archambeau, N. Méchitoua and M. Sakiz, "Code Saturne: a Finite Volume Code for the Computation of Turbulent Incompressible flows - Industrial Applications", IJFV International Journal On Finite Volumes, 1, 1-62, 2004.

[8] J. Mougenot, J.-J. Gonzalez, P. Freton *et al*, "Plasma-weld pool interaction in tungsten inert-gas configuration", J. Phys. D: App. Phys., 46, 135206, 2013.